

# Quantifying proximal and distal sources of NO in asthma using a multicompartment model

David A. Shelley, James L. Puckett, and Steven C. George

Department of Chemical Engineering and Materials Science and Department of Biomedical Engineering, University of California, Irvine, Irvine, California

Submitted 21 July 2009; accepted in final form 15 January 2010

**Shelley DA, Puckett JL, George SC.** Quantifying proximal and distal sources of NO in asthma using a multicompartment model. *J Appl Physiol* 108: 821–829, 2010. First published January 21, 2010; doi:10.1152/jappphysiol.00795.2009.—Nitric oxide (NO) is detectable in exhaled breath and is thought to be a marker of lung inflammation. The multicompartment model of NO exchange in the lungs, which was previously introduced by our laboratory, considers parallel and serial heterogeneity in the proximal and distal regions and can simulate dynamic features of the NO exhalation profile, such as a sloping phase III region. Here, we present a detailed sensitivity analysis of the multicompartment model and then apply the model to a population of children with mild asthma. Latin hypercube sampling demonstrated that ventilation and structural parameters were not significant relative to NO production terms in determining the NO profile, thus reducing the number of free parameters from nine to five. Analysis of exhaled NO profiles at three flows (50, 100, and 200 ml/s) from 20 children (age 7–17 yr) with mild asthma representing a wide range of exhaled NO (4.9 ppb < fractional exhaled NO at 50 ml/s < 120 ppb) demonstrated that 90% of the children had a negative phase III slope. The multicompartment model could simulate the negative phase III slope by increasing the large airway NO flux and/or distal airway/alveolar concentration in the well-ventilated regions. In all subjects, the multicompartment model analysis improved the least-squares fit to the data relative to a single-path two-compartment model. We conclude that features of the NO exhalation profile that are commonly observed in mild asthma are more accurately simulated with the multicompartment model than with the two-compartment model. The negative phase III slope may be due to increased NO production in well-ventilated regions of the lungs.

nitric oxide; heterogeneity; sensitivity; phase III slope

NITRIC OXIDE (NO) is a free radical present in exhaled breath and is thought to be a marker of inflammation in the lungs (3, 21). Exhaled NO can be elevated in inflammatory diseases, such as asthma, and is reduced after treatment with inhaled corticosteroids (ICS) (17). These observations have generated significant interest in the clinical use of exhaled NO as a noninvasive marker to diagnose and monitor the progression of inflammatory diseases.

Elevated NO in asthma has been traditionally attributed to inflammation in the proximal airways; however, recent evidence highlights the importance of peripheral regions (e.g., respiratory bronchioles) in inflammation (13, 18, 19). Elevated peripheral NO has been associated with increased symptoms and can be resistant to ICS (13). When NO is measured at the mouth during exhalation, the only way to distinguish between the proximal and peripheral NO sources is through a mathe-

tical model. The two-compartment model of NO exchange is a relatively simple, yet powerful, tool to partition the NO signal into proximal (large airways) and distal (small airways and alveoli) components (10, 32, 33, 43, 44). The two-compartment model separates the lung into a rigid trumpet-shaped airway region characterized by a constant NO production (or flux of NO from the airway wall surface) and an expansile distal airway/alveolar region characterized by a steady-state NO concentration. This model has been used to estimate proximal and distal NO sources in healthy subjects as well as numerous disease states, including asthma (13, 27, 35–39, 42).

Because of the single-path nature of the two-compartment model, there are inherent limitations in describing lung diseases such as asthma. The ventilation patterns in asthma are patchy and bimodal, with well-ventilated regions and poorly ventilated defect regions (45, 46). Our group recently developed the multicompartment model to account for regional heterogeneity in ventilation and NO production by adding a single branch point to the two-compartment model (41). Hence, the multicompartment model can simulate serial (or longitudinal) and parallel heterogeneity in ventilation and NO production and, thus, potentially provide a more accurate description of features in the exhaled NO profile that are not accounted for in the two-compartment model, such as a sloping phase III region (41). The improved accuracy is achieved at the cost of introducing additional free parameters, which can limit identification of the parameter space.

Our objective in the present study is to apply a rigorous sensitivity analysis to the multicompartment model and identify a subset of input parameters with a significant impact on model outputs, such as exhaled NO concentration and the slope of the phase III region. This information can be used to analyze experimental exhaled NO profiles of children with mild asthma, with the goal of assessing the potential of the multicompartment model to describe regional heterogeneity in NO production.

## Glossary

$\alpha$	Fraction of the total cross section at the branch point in the multicompartment model assigned to <i>compartment 1</i>
$A_i(z)$	Total cross-sectional area of the airway at location $z$ in <i>compartment i</i> ( $i = 0, 1, 2$ ) (cm <sup>2</sup> )
$\beta_{i,j}$	Partial rank correlation coefficient in Latin hypercube sampling multiple linear regression
$C_{ANO}$	Mean steady-state alveolar NO concentration for the two-compartment or the multicompartment model (ppb)
$C_{ANO,i}$	Steady-state NO concentration in alveolar <i>compartment i</i> of the multicompartment model ( $i = 1, 2$ ) (ppb)

Address for reprint requests and other correspondence: S. C. George, Dept. of Biomedical Engineering, 2420 Engineering Hall, Univ. of California, Irvine, Irvine, CA 92697-2730 (e-mail: scgeorge@uci.edu).

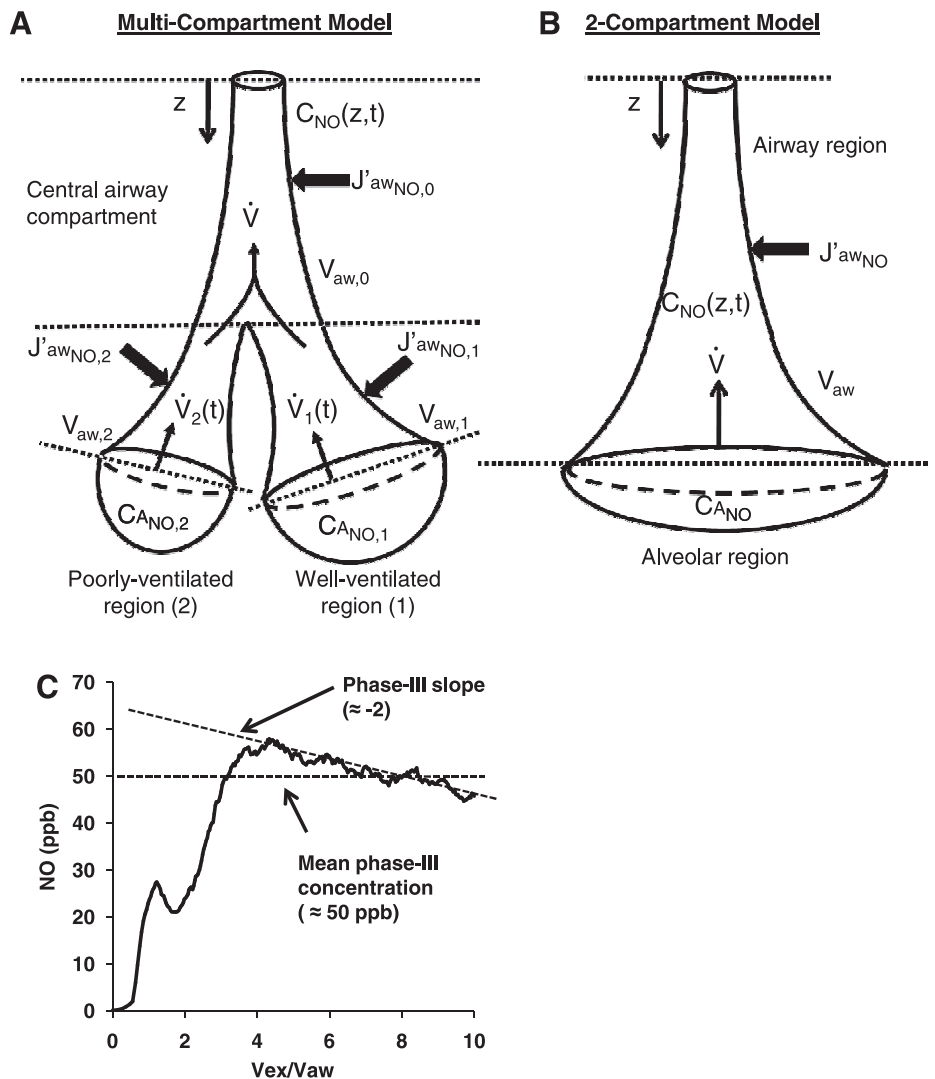
$C_{NO}(z,t)$	Concentration of NO in the airways at time $t$ , location $z$ (ppb)	$\dot{V}_{i,\infty}$	Steady-state flow ( $t = \infty$ ) in airway compartment $i$ ( $i = 1, 2$ )
$\bar{C}_{NO,III}$	Mean phase III NO plateau concentration (ppb)	$V_{aw}$	Total airway volume (ml)
$D$	Molecular diffusivity of NO in air	$V_{aw,i}$	Airway volume in compartment $i$ ( $i = 0, 1, 2$ ) (ml)
$F_{E_{NO,50}}$	Fractional exhaled NO at 50 ml/s (ppb)	$V_{ex}$	Cumulative exhaled volume (ml)
$FEV_1$	Forced expiratory volume in 1 s (%predicted)	$Y_{LS}$	95% confidence interval of parameter estimation
$FVC$	Forced vital capacity		
$J'_{awNO}$	Maximum total airway NO flux for the two-compartment or the multicompartment model (pl/s)		
$J'_{awNO,i}$	NO flux in airway compartment $i$ for the multicompartment model ( $i = 0, 1, 2$ ) (pl/s)		
$n$	Number of data points		
$p$	Number of free parameters		
RSS	Residual sum of squares of error between data and model predictions		
$\bar{S}_{NO,III}$	Phase III slope of NO exhalation		
$\tau$	Characteristic time constant of $\dot{V}_i(t)$ (s)		
$\dot{V}$	Total exhalation flow (ml/s)		
$\dot{V}_i(t)$	Flow in airway compartment $i$ at time $t$ ( $i = 1, 2$ ) (ml/s)		
$\dot{V}_{i,0}$	Initial flow ( $t = 0$ ) in airway compartment $i$ ( $i = 1, 2$ )		

## METHODS

**Model development.** Our group recently published a complete description of the multicompartment model of NO dynamics in the lung (41), and only the salient features are repeated here. The model consists of a central airway compartment that branches into two peripheral airway compartments that empty into separate alveolar regions (Fig. 1A). The airway regions have a trumpet-shaped geometry based on the anatomic measurements of Weibel (49), where the total volume approximates generations 1–16 (~175 ml). Hence, the linear dimension  $z$  of the model can be scaled for alternate total airway volume ( $V_{aw}$ ) using  $(V_{aw}/175)^{1/3}$ , with the constraint that the length-to-diameter ratio at any position within the trumpet is held constant. The governing equation is an unsteady diffusion-convection equation that can be solved numerically

$$\frac{\partial C}{\partial t} + \frac{\dot{V}_i(t)}{A_i(z)} * \frac{\partial C}{\partial z} = \frac{D}{A_i(z)} * \frac{\partial}{\partial z} \left[ A_i(z) * \frac{\partial C}{\partial z} \right] + \frac{J'_{awNO}}{V_{aw,i}} \quad (1)$$

Fig. 1. Schematic of the multicompartment and 2-compartment models of nitric oxide (NO) exchange in the lungs. **A:** multicompartment model consists of a central airway compartment that branches into 2 peripheral airway compartments, each emptying into separate alveolar regions. Each airway region is trumpet-shaped, incorporates axial diffusion, and has a constant NO flux per unit volume; alveolar compartments have a steady-state NO concentration. **B:** 2-compartment model consists of a single trumpet-shaped airway compartment with axial diffusion and constant NO flux per unit volume that empties into a single alveolar compartment that is at constant NO concentration. **C:** exhaled NO concentration in a representative child with asthma plotted as a function of exhaled airway volumes [exhaled volume ( $V_{ex}$ )/airway volume ( $V_{aw}$ ), unitless]. Key features include mean NO concentration of phase III (~50 ppb) and the phase III slope (approx -2 ppb). See *Glossary* for abbreviations.



where  $i = 0, 1, \text{ or } 2$  for the three airway compartments. The remaining parameters are defined in the *Glossary*. For the lower airway compartments ( $i = 1, 2$ ), the flow is given by

$$\dot{V}_i(t) = (\dot{V}_{i,0} - \dot{V}_{i,\infty})e^{-t/\tau} + \dot{V}_{i,\infty} \quad (2)$$

while the flow in the central compartment is the sum of the lower compartment flows

$$\dot{V} = \dot{V}_1(t) + \dot{V}_2(t) \quad (3)$$

This structure allows for heterogeneous ventilation in the lower airway compartments, while a constant exhalation flow at the mouth is maintained, as demonstrated previously (41).

The model can be used to simulate heterogeneity in ventilation and NO production as a function of nine independent parameters: five NO production terms ( $J'_{\text{awNO},0}$ ,  $J'_{\text{awNO},1}$ ,  $J'_{\text{awNO},2}$ ,  $C_{\text{ANO},1}$ , and  $C_{\text{ANO},2}$ ), three ventilation parameters ( $\dot{V}_{1,0}$ ,  $\dot{V}_{1,\infty}$ , and  $\tau$ ), and one structural parameter ( $\alpha$ ). The multicompartment model will be compared with the two-compartment model (Fig. 1B), which has been previously presented in detail (10, 34, 43) and is characterized by a rigid single-path trumpet representing the proximal airways in series with an expansile distal airway/alveolar region.

**Latin hypercube sampling.** Latin hypercube sampling (LHS) is a numerical simulation technique similar to Monte Carlo, but it is computationally more efficient and, thus, better suited for analysis of a nonlinear model with multiple unknown parameters (22). We previously utilized this method to characterize other models of gas exchange and NO dynamics (8, 40). Each model input is assigned a central value based on the literature, as well as an uncertainty range. For this study, we utilized 100 consecutive model simulations to achieve greater statistical significance. Each model input was divided into 100 equally probable values, where the mean is the central value and the range (minimum and maximum value) is the central value plus or minus the uncertainty. Each model simulation utilized a random selection of the input parameters without replacement; thus, for each of the 100 simulations, the set of input parameters was unique.

The results of LHS can be used to determine a sensitivity index for each of the input parameters and allow identification of inputs that have the greatest impact on the model outputs. The sensitivity index of each parameter is the partial rank correlation coefficient ( $\beta$ ) and is defined by the following relationship

$$Y_i^k = \lambda + \beta_{i,1}X_1^k + \beta_{i,2}X_2^k + \dots + \beta_{i,9}X_9^k \quad (4)$$

where  $Y$  is the value of the model output,  $\lambda$  is a constant,  $X$  is the value for the model input parameter,  $k$  is the simulation number, and  $i$  is the specific model output or input. All model outputs and inputs are normalized by the central or mean value, and then multiple linear regression is used to determine the values of  $\beta$ ; 95% confidence intervals are used to determine whether the values are statistically different from zero. In other words, LHS approximates a nonlinear model with a linear function in which each of the model inputs is normalized, such that magnitudes can be compared directly. Model outputs for this simulation include the NO plateau concentration, ( $C_{\text{NO,III}}$ ) and the phase III NO slope ( $S_{\text{NO}}^{\text{III}}$ ), as shown in Fig. 1C (10, 44).

Central values and uncertainty ranges for input parameters were estimated on the basis of the literature (Table 1). Structural and ventilation parameters were bounded, such that the well-ventilated unit emptied early in expiration (lower resistance) relative to the poorly ventilated unit (24, 25). These ventilation conditions produce a positive phase III slope for inert gas (e.g.,  $\text{N}_2$ ) washout simulations, as shown previously (41). NO parameters were divided into two groups, low  $\text{FE}_{\text{NO},50}$  (<25 ppb) and high  $\text{FE}_{\text{NO},50}$  (>25 ppb), on the basis of the upper limit of normal for children (7). The low- and high- $\text{FE}_{\text{NO}}$  simulations utilized a total airway NO flux of 1 and 6 nl/s, respectively (13, 17, 27, 29, 37). Uncertainty for the NO flux was chosen, such that the simulations covered the entire range of possible NO production for

Table 1. Latin hypercube sampling input parameters

	Central Value	Uncertainty	Source
$J'_{\text{awNO}}$ (Low $\text{FE}_{\text{NO},50}$ )	1 nl/s	100%	(13, 27, 29, 37)
$J'_{\text{awNO}}$ (High $\text{FE}_{\text{NO},50}$ )	6 nl/s	60%	(13, 17, 27)
$C_{\text{ANO}}$	6 ppb	100%	(12, 13, 18, 19, 27–29, 37)
$\dot{V}_{i,0}$	0.75	30%	
$\dot{V}_{i,\infty}$	0.3	100%	(5, 14, 24–26, 45, 46)
$\tau$	15	100%	
$\alpha$	0.75	30%	

low (0–2 nl/s) and high (2–10 nl/s) cases. The central value for alveolar NO concentration was held constant at 6 ppb, with an uncertainty of 100%, to simulate the range of NO values reported in the literature (12, 13, 18, 19, 27–29, 37).

**Experimental exhaled NO in children with asthma.** Twenty (13 male) children with mild asthma were enrolled in the study (Table 2). Each subject presented to the Children's Hospital of Orange County Breathmobile for an asthma evaluation. Criteria for the diagnosis of asthma included a previous history of recurrent coughing, wheezing, shortness of breath (at rest or after exercise), and symptomatic improvement following use of a short-acting bronchodilator. Patients were excluded from the study if they had any other heart or lung disease, smoked within the past 5 yr, or were treated with ICS for <8 wk. Short- and long-acting  $\beta_2$ -agonists were withheld for 12 h before the study. Average age was 12 (range 7–17) yr, and average height was 148 (range 125–173) cm.

Skin prick tests were performed by the nurse and assessed by the physician. The skin prick test revealed atopy to common aeroallergens (cat, dog, feathers, cockroach, dust mites, mold, weeds, trees, and grasses), and the patient was considered atopic if skin prick test was positive for at least one antigen. ICS-naïve subjects ( $n = 5$ ) were those who received no oral corticosteroids or ICS within the last 8 wk and ICS-treated subjects ( $n = 15$ ) were those who were treated with prescribed ICS for  $\geq 8$  wk. Atopic status and ICS use for each individual are indicated in Tables 4 and 5. In addition, asthma symptoms were quantified using the validated Asthma Control Test (ACT). The child version of the ACT is used for young (6- to 11-yr-old) children (20), and the adult version is used for older (12- to 17-yr-old) children, as recommended (23). An ACT score of  $\geq 20$  is indicative of good asthma control (see Tables 4 and 5).

For exhaled NO, subjects performed constant-exhalation maneuvers at three flows (50, 100, and 200 ml/s) performed in triplicate according to guidelines established by the American Thoracic Society (ATS) and the European Respiratory Society (ERS) (1). Subjects exhaled against a positive pressure to prevent nasal contamination. NO was measured by chemiluminescence (NIOX Flex, Aerocrine, Stockholm, Sweden). A criterion for eliminating a maneuver from the analysis was a coefficient of variation in the flow >5% over the analysis interval. Mean  $\text{FE}_{\text{NO}}$  at 50, 100, and 200 ml/s was 33 (range 5–120), 19 (range 3–74), and 11 (range 2–40) ppb, respectively. Subjects then performed standard spirometry (WinDx Spirometer, Creative Biomedics International) following ATS criteria (2). Average  $\text{FEV}_1$  (%predicted) was 109, with an  $\text{FEV}_1/\text{FVC}$  of 88%. The protocol was approved by the Institutional Review Board of the University of California, Irvine.

**Model fitting and confidence regions.** The model-governing equations were discretized, and a nonlinear least-squares fitting routine was utilized to approximate the model input values needed to achieve a best fit with the subject's exhaled NO profiles. Exhaled NO profiles are plotted as NO concentration (ppb) vs. total exhaled volume normalized by an estimate of the subject's airway volume; thus the  $x$ -axis represents airway volume turnover (10). Airway volume was estimated from the subject's height using the correlations presented by Kerr (16). The Weibel geometry was then scaled to each subject by

Table 2. Relative sensitivity coefficients (95% confidence intervals)

	Low F <sub>ENO,50</sub>		High F <sub>ENO,50</sub>	
	$\bar{C}_{NO,III}$	$\bar{S}_{NO}^{III}$	$\bar{C}_{NO,III}$	$\bar{S}_{NO}^{III}$
CA <sub>NO,1</sub>	0.45 (5%)	-0.58 (23%)	0.12 (13%)	-0.42 (33%)
CA <sub>NO,2</sub>	0.57 (4%)	0.56 (24%)	0.16 (10%)	0.44 (32%)
J' <sub>awNO,0</sub>	0.47 (5%)	0.0 (-)	0.76 (2%)	0.0 (-)
J' <sub>awNO,1</sub>	0.2 (12%)	-0.1 (154%)	0.36 (4%)	-0.27 (51%)
J' <sub>awNO,2</sub>	0.3 (8%)	0.0 (-)	0.49 (3%)	0.15 (96%)
$\dot{V}_{1,0}$	0.0 (-)	0.0 (-)	0.0 (-)	0.0 (-)
$\dot{V}_{1,\infty}$	0.0 (-)	0.04 (314%)	0.02 (79.2%)	0.16 (85%)
$\tau$	0.0 (-)	-0.06 (218%)	0.0 (-)	-0.22 (64%)
$\alpha$	0.04 (64%)	-0.03 (413%)	0.06 (25%)	-0.04 (327%)

the ratio of the subject's estimated airway volume to the Weibel airway volume. The plateau region of each of the subject's exhalations (3 flows) was fit simultaneously to the multicompartment model or the two-compartment model using nonlinear least-squares fitting to minimize the sum of squares of the error. Dispersion in the sampling tube was accounted for with convolution integrals of the model output using methods previously established (4, 11). In the multicompartment model fitting algorithm, the input parameters determined to be statistically insignificant on model outputs from the LHS simulations were set to their central values. Two-compartment model fits were achieved with the same algorithm used for the multicompartment model.

For both models, the 95% confidence regions ( $Y_{LS}$ ) for the estimated parameters were determined from

$$(Y_{LS} - \theta)^T \mathbf{P}^{-1} (Y_{LS} - \theta) = pF_{1-\alpha}(p, n - p) \quad (5)$$

where  $\theta$  is the estimated true value from the least-squares fit of the data,  $F_{1-\alpha}$  is the  $F$ -statistic for the number of parameters ( $p$ ) and the number of data points used ( $n$ ), and  $\mathbf{P}$  is the estimated covariance matrix (6, 44). The statistics toolbox in MATLAB was utilized to solve Eq. 5 for the confidence intervals in each simulation.

## RESULTS

**LHS.** Separate LHS simulations were performed for low- and high-F<sub>ENO</sub> conditions. The low-F<sub>ENO</sub> simulations (central value for  $J'_{awNO} = 1$  nl/s) produced a mean F<sub>ENO,50</sub> = 19 ppb, whereas the high-F<sub>ENO</sub> simulations (central value for  $J'_{awNO} = 6$  nl/s) produced a mean F<sub>ENO,50</sub> = 85 ppb. Partial rank correlation coefficients and 95% confidence intervals for low- and high-F<sub>ENO</sub> cases are presented in Table 3. Major findings include a strong positive correlation and small confidence interval (range 3–13%) for all five NO production terms on the mean exhaled NO concentration. As expected, the alveolar NO concentrations had a larger (and of equal magnitude) to the central airway compartment) impact on mean exhaled NO for low-F<sub>ENO</sub> simulations, while airway NO flux had the highest impact on mean exhaled NO for high-F<sub>ENO</sub> simulations. The phase III NO slope correlated positively to alveolar NO in the defect region (*region 2*) and negatively with alveolar NO in the well-ventilated region (*region 1*) for low- and high-F<sub>ENO</sub> conditions. Additionally, at high F<sub>ENO</sub>, the phase III slope correlated positively to airway NO flux in the defect region and negatively to airway NO flux in the well-ventilated region. Central airway NO flux had no impact on the phase III slope.

Ventilation parameters did not correlate with mean exhaled NO concentration for low or high F<sub>ENO</sub>, with the exception of a weak dependence on  $\alpha$ . For low F<sub>ENO</sub>, ventilation parameters

did not correlate with the phase III slope; for high F<sub>ENO</sub>, there was a weak dependence of the slope on  $\dot{V}_{1,0}$  and  $\tau$ . Relative to the magnitude of the NO production terms (range of absolute values 0.12–0.58, and 80% of the cases significantly different from zero), ventilation and structural parameters were essentially insignificant (range of absolute values 0.04–0.22, and 25% of the cases significantly different from zero) in determining the shape of the exhaled NO profiles. Furthermore, in no case did a ventilation parameter impact the concentration and the phase III slope for low or high F<sub>ENO</sub>. For this reason, the ventilation and structural parameters were set to their central values and held constant during parameter estimation.

**Model fitting.** No exhalation profiles were eliminated as a result of variability in the flow over the analysis interval. Representative NO profiles are presented in Fig. 2. F<sub>ENO</sub> is elevated in *subject 6* relative to healthy subjects, with an average (of the 3 flows) normalized phase III NO slope of -1.4% (Fig. 2A); F<sub>ENO</sub> is elevated in *subject 10*, with a more negative phase III slope of -2.2% (Fig. 2B). F<sub>ENO</sub> is low in *subject 12*, with an average normalized phase III slope of 0.2% (Fig. 2C), F<sub>ENO</sub> is low in *subject 18*, with a more negative phase III slope of -2.7% (Fig. 2D). The average exhaled NO concentration at each flow is plotted as a function of exhaled volume normalized by the subject's airway volume. For model-fitting purposes, the early portion of each exhalation was excluded from analysis because of instrumentation limitations. Briefly, each exhalation initially starts at a higher flow than desired and is followed by a short response time for the system to achieve a steady flow. This affects the initial portion of the exhaled profile, causing the concentration of NO to be lower than if the maneuver was performed at the targeted constant flow. We previously described this artifact in children in detail (30): from the start of exhalation to approximately exhaled airway turnover volumes of 4, 5, and 6 for flows of 50, 100, and 200 ml/s, respectively; thus those regions were not included in the model fitting. The criterion for selecting the true start of the exhalation profile was based on a zero rate of change in the flow with exhalation volume. The end of the plateau region was chosen as the point at which the flow decreased to >10% of target flow.

Table 3. Anthropomorphic data

Subject	Age (M/F)	Height (cm)	V <sub>aw</sub> (ml, predicted)
1	15 (M)	173	100
2	16 (M)	157	84
3	8 (F)	127	53
4	12 (M)	134	60
5	13 (M)	147	73
6	12 (M)	131	57
7	9 (M)	140	66
8	15 (M)	173	100
9	7 (M)	151	78
10	12 (M)	153	80
11	11 (F)	161	88
12	13 (M)	155	82
13	8 (M)	138	64
14	11 (F)	153	80
15	7 (M)	125	51
16	12 (M)	149	75
17	17 (F)	153	80
18	13 (F)	150	77
19	9 (F)	133	59
20	15 (M)	159	86

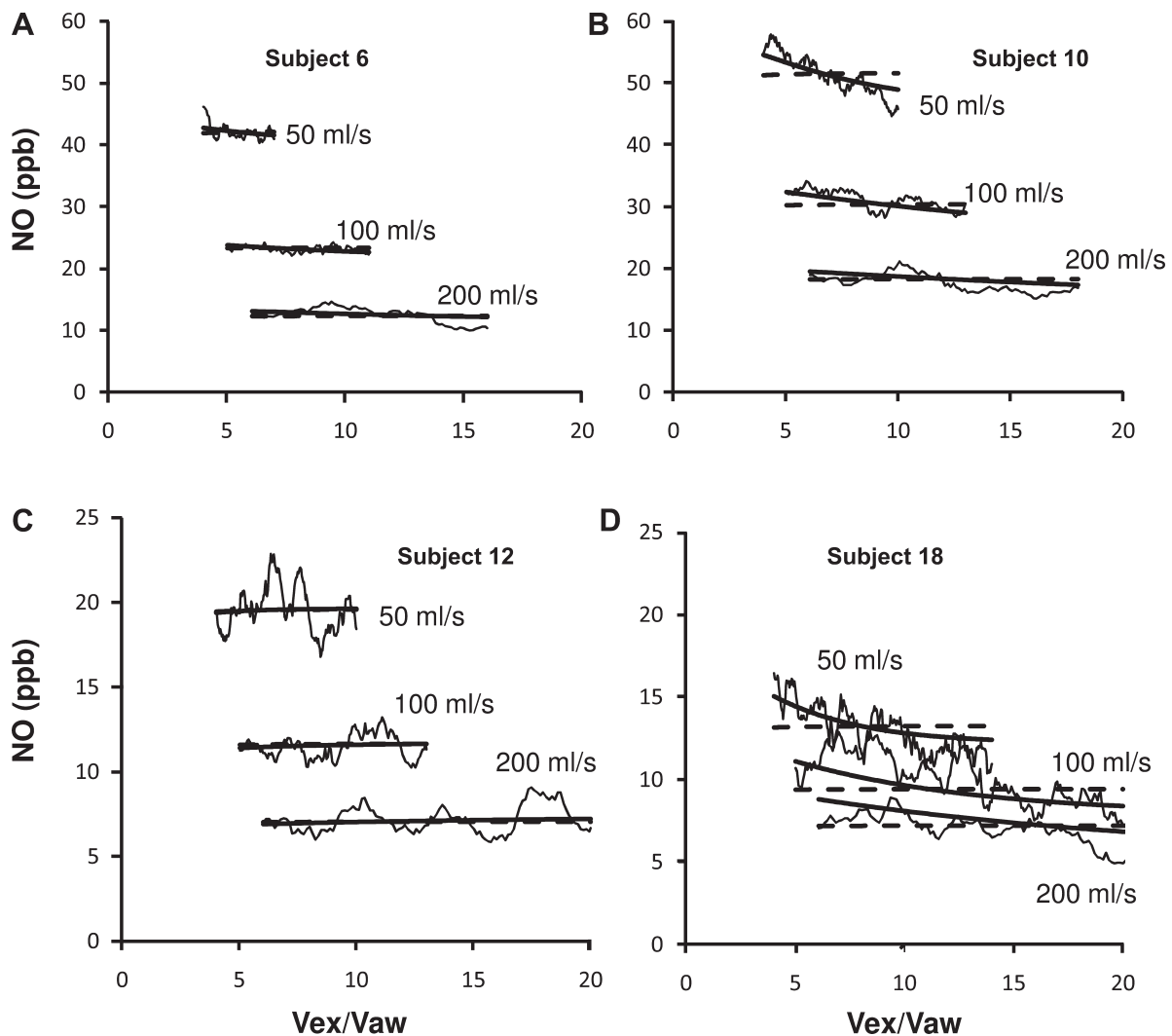


Fig. 2. Exhaled NO profiles and best-fit model simulations for 4 representative children with asthma. NO was collected at 3 exhalation flows (50, 100, and 200 ml/s) from 20 children with mild asthma. Exhaled NO in the phase III region of each flow is plotted as a function of the number of exhaled airway volumes (Vex/Vaw; thin trace). Multicompartment model best-fit curves are represented by a thick black line, and 2-compartment model best-fit curves are represented by dashed lines. *A*: *subject 6* has elevated  $F_{ENO}$  ( $>25$  ppb at a flow of 50 ml/s) with an average normalized phase III slope of  $-1.4\%$ . Multicompartment and 2-compartment model best fits are nearly identical. *B*: *subject 10* has elevated  $F_{ENO}$ , with an average normalized phase III slope of  $-2.2\%$ . *C*: *subject 12* has low  $F_{ENO}$ , with an average normalized slope of  $0.2\%$ . Multicompartment and 2-compartment model best fits are nearly identical. *D*: *subject 18* has low  $F_{ENO}$ , with a normalized phase III slope of  $-2.7\%$ .

A nonlinear least-squares fitting algorithm was utilized to approximate NO exchange parameters for the 20 subjects, with the ventilation parameters held constant at their central values, while the five NO parameters were simultaneously fit to the three exhalation curves. Each subject was fit to the two-compartment model and the multicompartment model; best-fit curves are presented in Fig. 2. Table 4 summarizes the NO parameter approximation of the two models for the 11 high- $F_{ENO}$  subjects, and Table 5 summarizes the parameter estimation for the 9 low- $F_{ENO}$  subjects. Tables 4 and 5 are sorted (high to low) by the average of the normalized phase III slope for each exhalation maneuver.

In general, the confidence intervals are smaller for the two-compartment model. The two-compartment model is able to predict  $J'_{awNO}$  and  $C_{ANO}$  with a confidence interval of  $<5\%$  and  $<50\%$ , respectively, with the exception of the near-zero alveolar concentrations in *subjects 4, 6, and 7*. For high- $F_{ENO}$

cases (Table 4), the addition of three parameters in the multicompartment model increases the confidence interval of all parameter estimations, with slightly less than half (25 of 55 or 45%) of the parameters having a confidence interval  $<100\%$ . Each subject in the high-NO category had statistically significant model predictions for  $J'_{awNO,1}$ , with the exception of *subject 4*. Of the 11 subjects with high NO, 6 had accurate predictions of  $J'_{awNO,0}$  and 7 had statistically significant estimations of  $C_{ANO,1}$ . Of the 11 high- $F_{ENO}$  cases, 9 were atopic, 3 were ICS naïve, 10 had a negative phase III slope, the average ACT score was 20.5, and the mean age was 11.8 (range 7–16) yr.

Low- $F_{ENO}$  cases (Table 5) had a slightly smaller rate of model parameter estimates with confidence intervals of  $<100\%$  (17 of 45, or 38%). For the low- $F_{ENO}$  cases, all subjects had statistically significant predictions for  $C_{ANO,1}$ , with the exception of *subject 20*, and two of the nine subjects had significant

Table 4. Parameter estimation and confidence intervals (high  $FE_{NO,50}$ )

Subject	$\bar{S}_{NO}^{III}$	ICS Naive	Atopic	ACT	Two-Compartment Model		Multi-Compartment Model				
					$J'_{awNO}$ , pl/s	$\bar{C}_{ANO}$ , ppb	$J'_{awNO,0}$ , nl/s	$J'_{awNO,1}$ , pl/s	$J'_{awNO,2}$ , pl/s	$C_{ANO,1}$ , ppb	$C_{ANO,2}$ , ppb
1	0.1	no	yes	21	2,570 (1%)	4.1 (7%)	40 (1,300%)	1,850 (20%)	1,130 (90%)	0.1 (1,300%)	5.4 (50%)
2	-0.1	no	yes	20	3,930 (1%)	2.7 (15%)	270 (340%)	2,660 (60%)	1,670 (160%)	0.1 (3,600%)	1.5 (370%)
3	-0.5	yes	no	19	2,780 (2%)	1.9 (21%)	650 (140%)	1,600 (60%)	570 (350%)	2.2 (100%)	1.7 (190%)
4	-1.2	yes	yes	19	3,190 (1%)	0.1 (300%)	1,500 (50%)	410 (220%)	670 (250%)	3.8 (70%)	0.1 (1,200%)
5	-1.3	no	yes	25	6,990 (1%)	1.3 (46%)	2,000 (50%)	3,520 (30%)	1,110 (180%)	6.7 (40%)	0.1 (3,500%)
6	-1.4	no	yes	22	3,450 (1%)	0.2 (150%)	1,370 (40%)	890 (40%)	660 (150%)	2.4 (60%)	0.1 (1,600%)
7	-1.5	no	yes	23	2,870 (1%)	0.1 (300%)	910 (70%)	1,460 (30%)	360 (320%)	0.1 (1,500%)	0.1 (2,500%)
8	-1.7	no	yes	18	9,430 (1%)	9.7 (9%)	240 (1,030%)	9,150 (30%)	2,830 (210%)	7.8 (80%)	0.2 (5,900%)
9	-1.8	no	yes	21	3,140 (1%)	0.9 (44%)	980 (80%)	1,390 (50%)	490 (320%)	4.3 (40%)	0.1 (2,700%)
10	-2.2	no	no	17	3,930 (2%)	3.9 (15%)	1,210 (60%)	2,280 (10%)	630 (180%)	4.5 (30%)	0.1 (2,400%)
11	-2.4	yes	yes	21	2,110 (2%)	1.6 (19%)	250 (280%)	2,250 (30%)	30 (4940%)	1.9 (80%)	0.1 (2,700%)

predictions for  $C_{ANO,2}$ . Six of the subjects had significant predictions for  $J'_{awNO,1}$ , and only one of the subjects had significant predictions for  $J'_{awNO,0}$ . The multicompartment model was able to identify at least one airway flux or distal airway/alveolar NO concentration in all 20 of the asthmatic subjects, regardless of the shape of the NO profile. Of the nine low- $FE_{NO}$  cases, five were atopic, two were ICS naïve, and eight had a negative phase III slope, the average ACT score was 18.9, and the mean age was 11.7 (range 8–17) yr.

**Model comparison.** The predicted total airway flux and average alveolar concentrations of the two-compartment model are compared with those of the multicompartment model in Fig. 3, A and B. Total airway flux ( $J'_{awNO}$ ) in the multicompartment model is the sum of the fluxes in each of the three branches, and the average alveolar concentration ( $C_{ANO}$ ) is a volume-weighted mean of the two alveolar concentrations (41).  $J'_{awNO}$  can be different in the multicompartment model and two-compartment model estimations; however, the differences are small and are not statistically (paired *t*-test,  $P > 0.05$ ) different.  $C_{ANO}$  is more variable between models, with some subjects exhibiting as much as a fivefold difference between the two model predictions. Nonetheless, there is no systematic bias, and the average  $C_{ANO}$  across all subjects was not statistically (paired *t*-test,  $P > 0.05$ ) different between the two models. Figure 3C is a plot of the percent improvement in RSS between the two-compartment model and the multicompartment model as a function of average normalized phase III slope of NO. In every subject, the multicompartment model achieves a better fit to the data than the two-compartment model, ranging from 1.5% to 65% improvement, with an average improvement of 22%. The phase III slope of NO correlated negatively with percent improvement of RSS.

## DISCUSSION

Our previous work presented the multicompartment model of NO exchange and demonstrated the importance of ventilation heterogeneity in describing features of the NO profile that cannot be accounted for with a single-path model, such as a sloping phase III region (41). The present study investigated the potential to identify the parameter space in the more advanced multicompartment model over a range of experimentally observed exhaled NO trends (high and low  $FE_{NO}$ , flat and sloping phase III) in children with mild asthma. The inclusion of parallel heterogeneity in ventilation and NO sources in the model allows for a nonzero slope in the exhaled NO concentration; however, variation in the magnitude of the parameters that characterize ventilation heterogeneity has little impact on the shape of the exhaled NO profile, whereas parameters describing the NO sources have a significant impact. Success in identifying the airway NO fluxes and distal airway/alveolar concentrations depends on the specific trend in the experimental exhaled NO profile. The multicompartment model may be particularly useful in identifying parallel heterogeneity (i.e., regional differences) in airway NO flux and distal airway/alveolar NO concentration in subjects with a significant phase III slope, which is not considered in ERS/ATS guidelines.

**Phase III slope.** Previous work from our group has shown that, in healthy patients, the phase III slope is statistically negative on average (43), as observed in the large majority (90%) of the children with mild asthma in the present study. Incorporation of parallel heterogeneities in ventilation and NO sources into the model creates a phase III slope. The magnitude of the phase III slope is controlled by a balance between the magnitude of NO production in the well-ventilated regions and the poorly ventilated regions. From LHS analysis, the phase III slope correlated posi-

Table 5. Parameter estimation and confidence intervals (low  $FE_{NO,50}$ )

Subject	$\bar{S}_{NO}^{III}$	ICS Naive	Atopic	ACT	Two-Compartment Model		Multi-Compartment Model				
					$J'_{awNO}$ , pl/s	$\bar{C}_{ANO}$ , ppb	$J'_{awNO,0}$ , nl/s	$J'_{awNO,1}$ , pl/s	$J'_{awNO,2}$ , pl/s	$C_{ANO,1}$ , ppb	$C_{ANO,2}$ , ppb
12	0.2	no	yes	21	1,410 (2%)	2.4 (8%)	430 (120%)	380 (120%)	390 (260%)	2.5 (40%)	3.6 (50%)
13	-1.2	no	yes	27	910 (2%)	0.7 (20%)	270 (110%)	360 (80%)	220 (250%)	1.7 (40%)	0.1 (980%)
14	-1.4	no	no	24	680 (2%)	1.1 (10%)	280 (90%)	160 (280%)	110 (600%)	2.4 (40%)	0.1 (1,400%)
15	-1.7	no	yes	18	1,180 (2%)	1.2 (20%)	340 (180%)	460 (80%)	340 (290%)	2.9 (40%)	0.1 (1,300%)
16	-1.7	yes	yes	10	450 (3%)	3.2 (4%)	170 (140%)	140 (150%)	100 (410%)	4.2 (20%)	1.6 (80%)
17	-2.1	no	no	12	320 (4%)	2 (5%)	70 (360%)	280 (80%)	60 (790%)	3.3 (20%)	0.1 (820%)
18	-2.7	no	yes	16	670 (4%)	5 (4%)	20 (1890%)	1,050 (30%)	10 (6930%)	7.6 (9%)	0.1 (1,300%)
19	-3.2	yes	no	24	350 (5%)	0.7 (20%)	90 (300%)	250 (80%)	30 (1,740%)	0.9 (70%)	0.1 (1,300%)
20	-6.9	no	no	18	440 (5%)	0.7 (30%)	60 (510%)	690 (30%)	20 (3,410%)	0.1 (860%)	0.1 (1,170%)

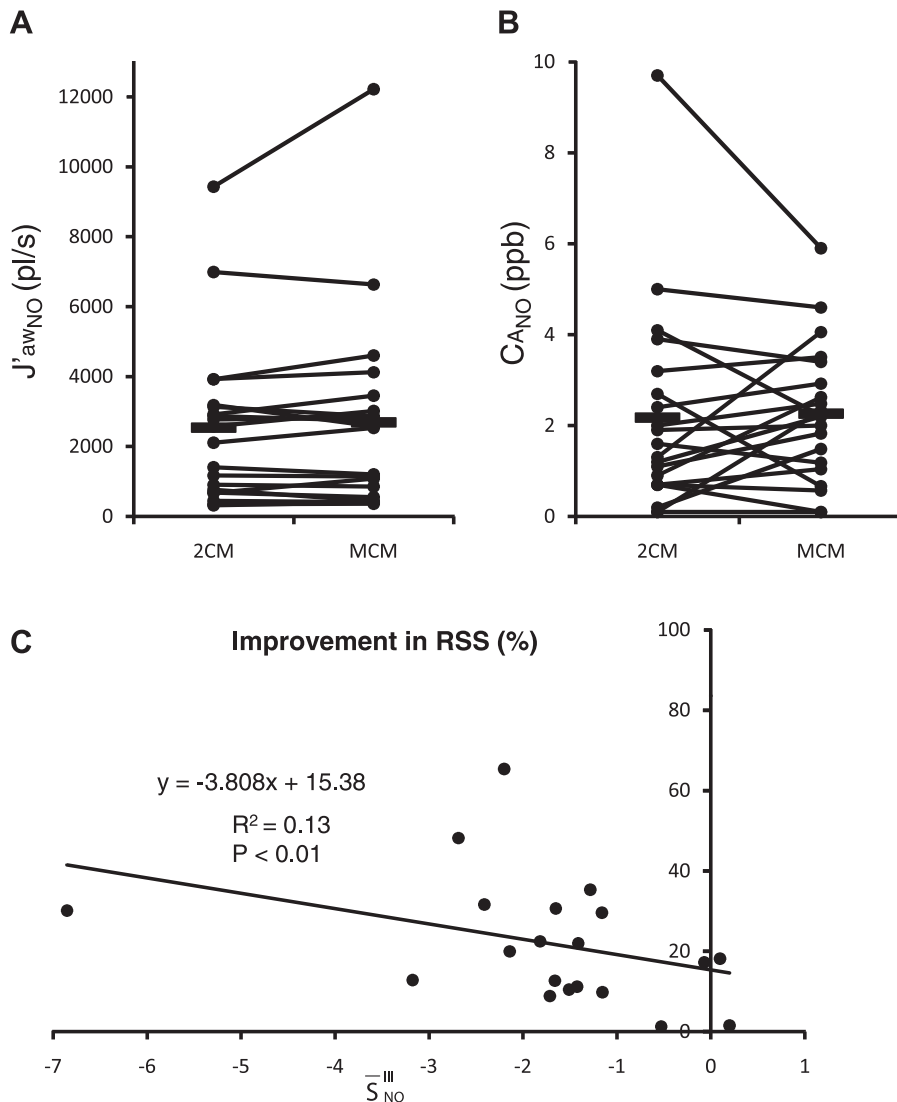


Fig. 3. Comparison of 2-compartment and multi-compartment models. *A*: total airway flux as determined by least-squares fitting the 2-compartment and multicompartment models to 20 children with asthma. Average predicted total airway NO flux for the multicompartment model was the sum of all 3 airway flux terms. *B*: average alveolar NO concentration determined by 2-compartment and multicompartment models. Average concentration was determined by volume weighting the 2 alveolar NO concentrations in the multicompartment model. Both models predicted similar NO levels on average (horizontal bars). *C*: percent improvement in residual sum of squares (RSS) between the 2-compartment and the multicompartment model as a function of the phase III slope of NO. There was a statistically significant negative correlation (solid line represents best-fit linear regression). See *Glossary* for abbreviations.

tively with NO in the poorly ventilated region and negatively with NO in the well-ventilated region. This is easy to understand, inasmuch as air from the well-ventilated region (*compartment* or *region 1* in the model) dominates the exhalate early in exhalation; hence, if the NO source in airway *compartment 1* or alveolar *region 1* is larger than that in the corresponding *compartment 2*, a negative phase III slope results. In other words, the multicompartment model predicts that a greater amount of NO arises from well-ventilated regions of the lung in most children with mild asthma. Although there are certainly patients with a positive phase III slope (41), our results suggest that a ventilation defect in a child with mild asthma is associated with decreased NO production in the same region.

One possible explanation for this observation is that an increased NO production serves to relax the smooth muscle by the well-characterized cGMP-dependent mechanism (9) and, thus, acts as an endogenous bronchodilator. Bronchodilation would lead to enhanced ventilation in regions of increased NO production. Venegas et al. (46) recently demonstrated that, even in a uniform airway tree model, a small perturbation in the smooth muscle is enough to cause dramatic ventilation inhomogeneities. In other words, a small perturbation in smooth muscle tone from

enhanced NO production could lead to significant changes in ventilation heterogeneity.

The multicompartment model presents only one mechanism for a negative phase III NO slope. As a subject expires from total lung capacity to functional residual capacity, the airway volume (generations 0–16) decreases. The decrease is small compared with the volume change in the distal compartments (generations 17–23) but may impact NO exchange dynamics. For example, during the course of an exhalation, the dynamic reduction in airway volume may decrease the surface area, emitting NO to the gas phase, leading to a decrease in exhaled NO with exhaled volume (i.e., a negative phase III slope). However, one might predict this effect to be mitigated by a reduced cross-sectional area for axial diffusion of NO (rate of axial diffusion is proportional to the cross-sectional area by Fick's first law of diffusion) and, thus, less NO lost to the alveolar region by "backdiffusion" (15, 32, 47, 48). Less NO lost to axial diffusion as exhalation proceeds would tend to create a positive phase III slope.

Serial heterogeneity in NO production and consumption within a distributed alveolar region (31) could also impact the phase III slope. For example, a progressively increasing density of alveoli

in generations 17–23 (49) (rather than the current well-mixed compartment) could cause an axial gradient in NO consumption in these regions from low consumption (generation 17) to high consumption (generation 23), leading to a negative phase III slope. However, the increasing density of alveoli would also lead to an increase in NO production and a positive phase III slope, thus offsetting the impact of consumption.

**Model identification: multicompartment model vs. two-compartment model.** In our 20 children with mild asthma, the multicompartment model was able to identify one to three of the five NO parameters (average ~40%, or 2 of the 5). This is the same number of free parameters in the two-compartment model. However, because most subjects had a negative phase III slope, the multicompartment model predicted a regional imbalance in NO production weighted toward one or more of the airway compartments, the alveolar compartments, or both. In all but two subjects (*subjects 1 and 12*), the imbalance was weighted toward the well-ventilated region, as would be predicted by a negative phase III slope. For *subjects 1 and 12*, the average phase III slope was flat or slightly positive. Both were treated with ICS and were atopic; the two-compartment and multicompartment models predicted an elevated level of distal NO in both subjects.

Parameter estimation in the multicompartment model can potentially be improved with additional NO data collected from each subject. This study utilized exhaled NO at multiple flows, similar to previous studies utilizing the two-compartment model (10, 43, 47). However, addition of three additional model parameters to describe the same data set accounts for the increase in confidence intervals. This effect could be minimized with additional or a wider range of maneuvers (e.g., breath hold) or exhalation flows (33, 44). For example, at 50 ml/s, the exhaled NO signal is primarily due to the airway regions, and thus a positive or negative slope at low flows can be modeled by increased NO in one of the airway compartments. As the flow is increased, the alveolar region accounts for a higher percentage of the exhaled signal, and thus the phase III slope at higher flows can be modeled with increased NO in one of the distal airway/alveolar regions. When *subject 10* is used as an example (Fig. 2B), the phase III slope at 50 ml/s is highly negative, but it is significantly less negative at the higher flows. These features are accounted for with an elevated NO production in the well-ventilated airway region and alveolar region relative to the poorly ventilated regions. On the other hand, *subject 12* (Fig. 2C) has a relatively flat slope at every flow; the parameter estimation places equivalent levels of NO in every airway compartment, none of which are statistically significant. In this case, no more information is provided by the multicompartment model than by the two-compartment model. Thus the choice of exhalation flows and maneuvers may not only improve the confidence intervals of parameter estimates, but the optimal choice may depend on the subject.

**Regional elevation in NO production.** The critical feature of the multicompartment model is its ability to distinguish a region of increased NO production, which may reflect increased inflammation in a disease such as asthma. Although standards for techniques and cut points for the upper limit of normal have not been established, several examples in our limited study of 20 children with mild asthma are worth discussion. Of particular interest is the alveolar concentration, which has been associated with enhanced symptoms (13, 18, 19). For the high-F<sub>ENO</sub> cases, *subjects 4, 5, and 9* had C<sub>ANO</sub> values of 0.1, 1.3, and 0.9 ppb predicted by the two-compartment model, but C<sub>ANO,1</sub> as predicted

by the multicompartment model was 3.8, 6.7, and 4.3 ppb. Although not as dramatic, a similar trend can be observed in two of the low-F<sub>ENO</sub> subjects (*subjects 14 and 15*), in which C<sub>ANO</sub> from the two-compartment model was 1.1 and 1.2 ppb and C<sub>ANO,1</sub> from the multicompartment model increased to 2.4 and 2.9 ppb. Thus the multicompartment model may have utility in identifying an elevated regional alveolar concentration of NO that cannot be detected by the two-compartment model.

**Conclusions.** The multicompartment model of NO exchange incorporates parallel heterogeneity in ventilation and NO production and, thus, can predict a sloping phase III in the NO exhalation profile, a situation that occurs in the large majority of children with mild asthma but cannot be simulated with the single-path two-compartment model and is not considered in ATS/ERS guidelines. The added complexity increases the number of free parameters in the model from two to nine; however, our sensitivity analysis predicts that only five parameters describing NO sources are critical in characterizing the NO exhalation profile. Furthermore, when the model is applied to the same set of data as the two-compartment model, ~40% (2 of 5) of the free parameters of the multicompartment model can be accurately determined, the same number of free parameters in the two-compartment model. To simulate the negative phase III slope, the multicompartment model predicts a parallel imbalance in NO production weighted toward the well-ventilated large airway and small airway/alveolar regions. Hence, the multicompartment model may alter the definition and interpretation of elevated NO production in the lungs. Future studies must examine larger and more diverse populations of children and adults with asthma and other inflammatory lung diseases and explore additional exhalation flows and breathing maneuvers to further define the utility of the multicompartment model.

#### ACKNOWLEDGMENTS

We thank the staff and director (Dr. Stanley Galant) of the Children's Hospital of Orange County Breathmobile.

#### GRANTS

This work was supported by National Institutes of Health Grants HL-070645 and RR-00827.

#### DISCLOSURES

No conflicts of interest are declared by the author(s).

#### REFERENCES

1. **American Thoracic Society/European Respiratory Society.** Recommendations for standardized procedures for the online and offline measurement of exhaled lower respiratory nitric oxide and nasal nitric oxide. *Am J Respir Crit Care Med* 171: 912–930, 2005.
2. **American Thoracic Society.** Lung function testing: selection of reference values, and interpretative strategies. *Am Rev Respir Dis* 144: 1202–1218, 1991.
3. **Alving K, Weitzberg E, Lundberg JM.** Increased amount of nitric oxide in exhaled air of asthmatics. *Eur Respir J* 6: 1368–1370, 1993.
4. **Aris R.** *Elementary Chemical Reactor Analysis*. Boston: Butterworths, 1989, p. xii, 352.
5. **Bates JH, Rossi A, Milic-Emili J.** Analysis of the behavior of the respiratory system with constant inspiratory flow. *J Appl Physiol* 58: 1840–1848, 1985.
6. **Beck JV, Arnold KJ.** *Parameter Estimation in Engineering and Science*. New York: Wiley, 1977, p. xix, 501.
7. **Buchvald F, Baraldi E, Carraro S, Gaston B, De Jongste J, Pijnenburg MW, Silkoff PE, Bisgaard H.** Measurements of exhaled nitric oxide in healthy subjects age 4 to 17 years. *J Allergy Clin Immunol* 115: 1130–1136, 2005.

8. Bui TD, Dabdub D, George SC. Modeling bronchial circulation with application to soluble gas exchange: description and sensitivity analysis. *J Appl Physiol* 84: 2070–2088, 1998.
9. Condorelli P, George SC. In vivo control of soluble guanylate cyclase activation by nitric oxide: a kinetic analysis. *Biophys J* 80: 2110–2119, 2001.
10. Condorelli P, Shin HW, Aledia AS, Silkoff PE, George SC. A simple technique to characterize proximal and peripheral nitric oxide exchange using constant flow exhalations and an axial diffusion model. *J Appl Physiol* 102: 417–425, 2007.
11. Condorelli P, Shin HW, George SC. Characterizing airway and alveolar nitric oxide exchange during tidal breathing using a three-compartment model. *J Appl Physiol* 96: 1832–1842, 2004.
12. Geigel EJ, Hyde RW, Perillo IB, Torres A, Perkins PT, Pietropaoli AP, Frasier LM, Frampton MW, Utell MJ. Rate of nitric oxide production by lower alveolar airways of human lungs. *J Appl Physiol* 86: 211–221, 1999.
13. Gelb AF, Taylor CF, Nussbaum E, Gutierrez C, Schein A, Shinar CM, Schein MJ, Epstein JD, Zamel N. Alveolar and airway sites of nitric oxide inflammation in treated asthma. *Am J Respir Crit Care Med* 170: 737–741, 2004.
14. Harris RS, Winkler T, Tgavalekos N, Musch G, Melo MF, Schroeder T, Chang Y, Venegas JG. Regional pulmonary perfusion, inflation, and ventilation defects in bronchoconstricted patients with asthma. *Am J Respir Crit Care Med* 174: 245–253, 2006.
15. Kerckx Y, Michils A, Van Muylem A. Airway contribution to alveolar nitric oxide in healthy subjects and stable asthma patients. *J Appl Physiol* 104: 918–924, 2008.
16. Kerr AA. Dead space ventilation in normal children and children with obstructive airways disease. *Thorax* 31: 63–69, 1976.
17. Kharitonov SA, Yates DH, Chung KF, Barnes PJ. Changes in the dose of inhaled steroid affect exhaled nitric oxide levels in asthmatic patients. *Eur Respir J* 9: 196–201, 1996.
18. Lehtimäki L, Kankaanranta H, Saarelainen S, Turjanmaa V, Moilanen E. Increased alveolar nitric oxide concentration in asthmatic patients with nocturnal symptoms. *Eur Respir J* 20: 841–845, 2002.
19. Lehtimäki L, Kankaanranta H, Saarelainen S, Turjanmaa V, Moilanen E. Peripheral inflammation in patients with asthmatic symptoms but normal lung function. *J Asthma* 42: 605–609, 2005.
20. Liu AH, Zeiger R, Sorkness C, Mahr T, Ostrom N, Burgess S, Rosenzweig JC, Manjunath R. Development and cross-sectional validation of the Childhood Asthma Control Test. *J Allergy Clin Immunol* 119: 817–825, 2007.
21. Mattes J, Storm van's Gravesande K, Reining U, Alving K, Ihorst G, Henschen M, Kuehr J. NO in exhaled air is correlated with markers of eosinophilic airway inflammation in corticosteroid-dependent childhood asthma. *Eur Respir J* 13: 1391–1395, 1999.
22. McKay MD, Beckman RJ, Conover WJ. A comparison of three methods for selecting values of input variables in the analysis of output from a computer code. *Technometrics* 21: 239–245, 1979.
23. Nathan RA, Sorkness CA, Kosinski M, Schatz M, Li JT, Marcus P, Murray JJ, Pendergraft TB. Development of the Asthma Control Test: a survey for assessing asthma control. *J Allergy Clin Immunol* 113: 59–65, 2004.
24. Paiva M. Two new pulmonary functional indexes suggested by a simple mathematical model. *Respiration* 32: 389–403, 1975.
25. Paiva M, Engel LA. The anatomical basis for the sloping N<sub>2</sub> plateau. *Respir Physiol* 44: 325–337, 1981.
26. Paiva M, van Muylem A, Engel LA. Slope of phase III in multibreath nitrogen washout and washin. *Bull Eur Physiopath Respir* 18: 273–280, 1982.
27. Paraskakis E, Brindicci C, Fleming L, Krol R, Kharitonov SA, Wilson NM, Barnes PJ, Bush A. Measurement of bronchial and alveolar nitric oxide production in normal children and children with asthma. *Am J Respir Crit Care Med* 174: 260–267, 2006.
28. Perillo IB, Hyde RW, Olszowka AJ, Pietropaoli AP, Frasier LM, Torres A, Perkins PT, Forster RE 2nd, Utell MJ, Frampton MW. Chemiluminescent measurements of nitric oxide pulmonary diffusing capacity and alveolar production in humans. *J Appl Physiol* 91: 1931–1940, 2001.
29. Pietropaoli AP, Perillo IB, Torres A, Perkins PT, Frasier LM, Utell MJ, Frampton MW, Hyde RW. Simultaneous measurement of nitric oxide production by conducting and alveolar airways of humans. *J Appl Physiol* 87: 1532–1542, 1999.
30. Puckett JL, Taylor RWE, Galant SP, George SC. Impact of analysis interval on the multiple flow technique to partition exhaled nitric oxide. *Pediatr Pulmonol* 45: 182–191, 2010.
31. Scherer PW, Gobran S, Aukburg SJ, Baumgardner JE, Bartkowski R, Neufeld GR. Numerical and experimental study of steady-state CO<sub>2</sub> and inert gas washout. *J Appl Physiol* 64: 1022–1029, 1988.
32. Shin HW, Condorelli P, George SC. Examining axial diffusion of nitric oxide in the lungs using heliox and breath hold. *J Appl Physiol* 100: 623–630, 2006.
33. Shin HW, Condorelli P, George SC. A new and more accurate technique to characterize airway nitric oxide using different breath-hold times. *J Appl Physiol* 98: 1869–1877, 2005.
34. Shin HW, George SC. Impact of axial diffusion on nitric oxide exchange in the lungs. *J Appl Physiol* 93: 2070–2080, 2002.
35. Shin HW, Rose-Gottron CM, Cooper DM, Hill M, George SC. Impact of high-intensity exercise on nitric oxide exchange in healthy adults. *Med Sci Sports Exerc* 35: 995–1003, 2003.
36. Shin HW, Rose-Gottron CM, Cooper DM, Newcomb RL, George SC. Airway diffusing capacity of nitric oxide and steroid therapy in asthma. *J Appl Physiol* 96: 65–75, 2004.
37. Shin HW, Rose-Gottron CM, Perez F, Cooper DM, Wilson AF, George SC. Flow-independent nitric oxide exchange parameters in healthy adults. *J Appl Physiol* 91: 2173–2181, 2001.
38. Shin HW, Rose-Gottron CM, Sufi RS, Perez F, Cooper DM, Wilson AF, George SC. Flow-independent nitric oxide exchange parameters in cystic fibrosis. *Am J Respir Crit Care Med* 165: 349–357, 2002.
39. Shin HW, Schwindt CD, Aledia AS, Rose-Gottron CM, Larson JK, Newcomb RL, Cooper DM, George SC. Exercise-induced bronchoconstriction alters airway nitric oxide exchange in a pattern distinct from spirometry. *Am J Physiol Regul Integr Comp Physiol* 291: R1741–R1748, 2006.
40. Shin HY, George SC. Microscopic modeling of NO and S-nitrosoglutathione kinetics and transport in human airways. *J Appl Physiol* 90: 777–788, 2001.
41. Suresh V, Shelley DA, Shin HW, George SC. Effect of heterogeneous ventilation and nitric oxide production on exhaled nitric oxide profiles. *J Appl Physiol* 104: 1743–1752, 2008.
42. Suri R, Paraskakis E, Bush A. Alveolar, but not bronchial nitric oxide production is elevated in cystic fibrosis. *Pediatr Pulmonol* 42: 1215–1221, 2007.
43. Tsoukias NM, George SC. A two-compartment model of pulmonary nitric oxide exchange dynamics. *J Appl Physiol* 85: 653–666, 1998.
44. Tsoukias NM, Shin HW, Wilson AF, George SC. A single-breath technique with variable flow rate to characterize nitric oxide exchange dynamics in the lungs. *J Appl Physiol* 91: 477–487, 2001.
45. Venegas JG, Schroeder T, Harris S, Winkler RT, Melo MF. The distribution of ventilation during bronchoconstriction is patchy and bimodal: a PET imaging study. *Respir Physiol Neurobiol* 148: 57–64, 2005.
46. Venegas JG, Winkler T, Musch G, Vidal Melo MF, Layfield D, Tgavalekos N, Fischman AJ, Callahan RJ, Bellani G, Harris RS. Self-organized patchiness in asthma as a prelude to catastrophic shifts. *Nature* 434: 777–782, 2005.
47. Verbanck S, Kerckx Y, Schuermans D, de Bisschop C, Guenard H, Naeije R, Vincken W, Van Muylem A. The effect of posture-induced changes in peripheral nitric oxide uptake on exhaled nitric oxide. *J Appl Physiol* 106: 1494–1498, 2009.
48. Verbanck S, Kerckx Y, Schuermans D, Vincken W, Paiva M, Van Muylem A. Effect of airways constriction on exhaled nitric oxide. *J Appl Physiol* 104: 925–930, 2008.
49. Weibel ER. *Morphometry of the Human Lung*. Berlin: Springer, 1963, p. xi, 151.